View metadata, citation and similar papers at core.ac.uk
brought to you by CORE
provided by Queensland University of Technology ePrints Archive

COMPUTATIONAL ASPECTS OF PROBABILISTIC ASSESSMENT OF UAS ROBUST AUTONOMY

Tristan Perez[*,*], Brendan Williams[**], Pierre de Lamberterie[*]**
[*]School of Engineering, The University of Newcastle, Callaghan NSW 2308, AUSTRALIA,
[**]Boeing Research & Technology Australia, GPO Box 767 QLD-4001, AUSTRALIA,
[***] CeSOS, Norwegian University of Science and Technology, Trondheim, NORWAY
tristan.perez@newcastle.edu.au; brendan.p.williams@boeing.com;
pierre.delamberterie@uon.edu.au

Keywords: *Robust Autonomy, UAS design & certification*

Abstract

As the level of autonomy in Unmanned Aircraft Systems (UAS) increases, there is an imperative need for developing methods to assess robust autonomy. This paper focuses on the computations that lead to a set of measures of robust autonomy. These measures are the probabilities that selected performance indices related to the mission requirements and airframe capabilities remain within regions of acceptable performance.

1 Introduction

The large potential for applications of Unmanned Aircraft Systems (UAS) in civilian operations and national security is putting an increasing amount of pressure on National Airworthiness Authorities (NAAs) to provide a path for certification and allow UAS integration into the national airspace [1]. Decisions about certification must be based on demonstrated levels of varying degrees of robust autonomy.

In a companion paper [2], the authors describe a probabilistic framework for performance evaluation of UAS Robust Autonomy. This framework is akin to the evaluation that pilots undergo during the licensing process, and the data from the proposed evaluation can be used as an aid for decision making in certification and UAS designs. The outcomes of the performance evaluation are a set of measures of robust autonomy. These measures are the probabilities that performance indices related to the mission requirements and airframe capabilities remain within regions of acceptable performance. This paper discusses the computational aspects of the measures of robust autonomy.

2 Robust Autonomy of UAS and its Evaluation

Robust autonomy describes the ability of an autonomous system to either continue its operation in the presence of faults or safely shut down [2]. Robust autonomy encapsulates the reliability of the UAS physical platform and components plus the ability of autonomous decision making—to varying degrees—in relation to guidance, navigation, communications and control. In a manned aircraft, the decision making aspect rests entirely on the pilot, whereas a remotely operated aircraft the system must have certain degree of autonomy and the pilot monitors the operation and makes decisions only the case of an emergency.

It is important to highlight from the outset that when assessing humans for issuing a pilot license, we do not expect that each and every emergency situation will result in a satisfactory outcome. What is assessed is that the actions of the candidate pilot conform to accepted "best practices" and that the actions position the air-

craft in a manner that maximises the likelihood of a satisfactory outcome over an envelope of scenarios that simulate potential emergency situations. When assessing autonomy of UAS, we need to keep this in mind as the assessment cannot guarantee a positive outcome for each and every emergency scenario. The above suggest that the assessment of robust autonomy, as well as the assessment of pilots, involves making decisions under uncertainty. This calls for a probabilistic framework, which is the approach proposed in [2, 3, 4].

The performance of a UAS system can be assessed in essentially the same way as pilots are assessed. Within this framework the pilot being tested is replaced by proprietary hardware, and associated software, that implements the functions of decision making in relation to guidance, navigation, communications and control (GNCC). These functions can include fault detection & diagnosis and reconfiguration of the GNCC systems to accommodate faults and prevent system failure. The GNCC hardware is connected to a hardware-in-the-loop (HIL) simulation environment which can simulate different aspects of the mission under various environmental conditions and fault scenarios (sensors, actuators, UAS platform aerodynamics, other aircraft, etc.) The data collected from these HIL simulations can then be used to assess performance and therefore decision making about certification and system design. This process is illustrated in Figure 1.

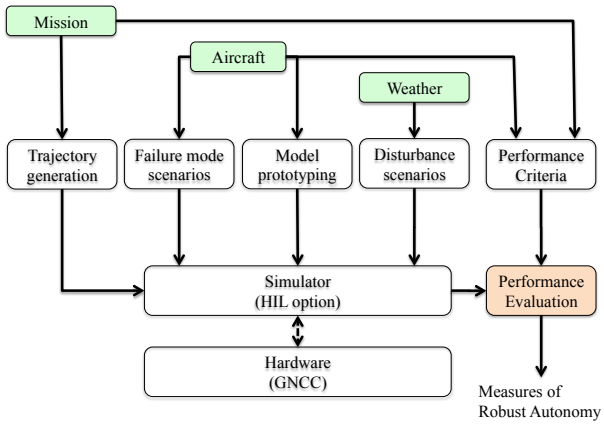

Fig. 1 Evaluation of Robust Autonomy.

2.1 Performance Criteria and Environment

UAS are specifically designed for particular missions and environments under which the missions need to be conducted. The measures of performance discussed in the previous section can be evaluated in terms of specific performance indices related to mission requirements and airframe capabilities. For example Table 1 shows some of the performance indices that can be adopted according to the measures of performance related to Aviate, Navigate, and Communicate.

Table 1 Example of performance indices for UAS Missions.

Index	Description
r_1	Climbing rate
r_2	Bank angle
r_3	Loading factor
r_4	Angle of attack
r_5	Sideslip angle
r_6	Air speed
r_7	Sense & avoid
r_8	Ability to land
r_9	Kinetic energy in emergency landing
r_{10}	Required location
r_{11}	Remain outside of a no-fly zone

For each index r_i $(i = 1,2,\ldots,l)$ we can associate set $\mathcal{R}_i$, such that satisfactory performance is attained whenever the value of the index is in the set $\mathcal{R}_i$ for the complete mission.

The mission is to be performed under an envelope of operational conditions that encompasses environmental conditions and faults. The environmental conditions $W_j\,(j = 1,2,\ldots,m)$ refer to weather such as wind velocity and turbulence. The uncertainty as to which environmental condition can occur during the mission is described by the probability $P(W_j|I)$, where I represents background information. These probabilities can be estimated from meteorological data for a particular geographical location and

time of the year. Note that the weather conditions to be considered for the operation of the UAS may depend on the type mission. For example, a UAS used for bush fire monitoring is expected to operate in high speed and highly turbulent winds, whereas a UAS used for aerial photography is expected to operate in light wind conditions.

The UAS platform may also be subjected to faults $F_k\,(k = 0,1,\ldots,n)$, which can be associates with actuators, sensors, communication link, changes in aerodynamics, and the presence of other aircraft. The fault F_0 denotes the faultless or healthy case. The uncertainty as to which fault may occur during the mission is described by the probability $P(F_k|I)$, where I represents background information. If the fault is associated with a component or a subsystem, for example a servo of a control surface, then $P(F_k|I)$ is can be taken as the reliability of the component or subsystem. That is $P(F_k|I)$ is the probability that the fault F_k will occur during the mission given that the fault has not occurred at the time of starting the mission. This probability is standard measure in reliability, and it can be computed from the failure rate function of the component or system [5].

2.2 Evaluating Performance

For each performance index, we can define the event of satisfactory performance as that in which a performance index remains inside its region of satisfactory performance for the complete mission:

$$S_i \equiv \{r_i \in \mathcal{R}_i\}. \tag{1}$$

Note, that S_i is an event that can be either true or false after a mission is evaluated.

The evaluation of the performance during the mission can be assessed in terms of the predicted probabilities of satisfactory performance of each index in one mission given what we have learned from the data D related to the evaluation of the system. These probabilities can be computed by magninalising over the operational conditions (weather and faults):

$$\begin{aligned} P(S_i|D,I) &= \sum_j \sum_k P(S_i,W_j,F_k|D,I) \qquad (2)\\ &= \sum_j \sum_k P(S_i|W_j,F_k,D)\,P(W_j|I)P(F_k|I). \end{aligned}$$

These probabilities are called *Measures of Robust Autonomy* [2]. Each of these measures involves different aspects of the system which contribute to its reliability:

- $P(W_j|I)$ and $P(F_k|I)$ capture uncertainty about the operational conditions of the system. $P(W_j|I),(j = 1 : m)$ define the envelope of environmental conditions and $P(F_k|I),(k = 1 : n)$ capture the reliability of the platform component and subsystems. Note that we are assuming that W_j and F_k are conditionally independent, namely, $P(W_j,F_k|I) = P(W_j|I)P(F_k|I)$.
- $P(S_i|W_j,F_k,D,I),(i = 1 : l)$ evaluates the quality of autonomous decision making in the GNCC systems of the UAS. This encompasses aspects of robustness and performance of the flight control system, fault detection and diagnosis system, and on-line decisions about reconfiguration of the flight control system and mission re-routing and trajectory planning.

The probabilities $P(S_i|W_j,F_k,D,I)$ are related to the concept of *coverage* discussed in [6], that is, the probability of keeping a desired level of performance given that a particular scenario (weather and fault) has occurred. In the context of this paper, coverage encompasses not only the low-level motion flight controller but, depending on the degree of autonomy of the platform, also the guidance and sense and avoid system.

The probabilities $P(S_i|D,I)$ in (2) are the predicting probabilities of success of the performance index remaining in their region of acceptable performance in one mission. This can be generalised to a cumulative probability of having at least a certain number of successes in a number of missions.

3 Computation of Coverage Probabilities

The evaluation of robust autonomy requires the computation of coverage probabilities based on data of experimental testing of GNCC hardware and software with a hardware-in-the-loop testing simulations. This computation can be separated into two parts: inference and prediction.

3.1 Inference

If satisfactory performance is defined in terms of the values of the performance indices being inside a particular range, $r_i \in \mathcal{R}_i$, the events defined in (1) are outcomes of Bernoulli trials, that is success or failure. Hence, if the system is tested a number of times N, for each index we have a sequence of binary results

$$D_i = \{s_i(1), s_i(2), \ldots, s_i(N)\}.$$

The probability of observing these data is given by the Bernoulli distribution:

$$p(D_i|\theta, I_{jk}) = \theta^R (1-\theta)^{N-R}, \tag{3}$$

where R represents the number of successes within the sequence D_i, θ represents the probability of success, that is $P(r_i \in \mathcal{R}_i)$ in one trial, and $I_{jk} = \{W_j, F_k, I\}$ represents the information related to the particular condition being tested. To estimate the parameter θ, we can follow a Bayesian approach and compute the posterior distribution of θ given the data from the test:

$$p(\theta|D_i, I_{jk}) = \frac{p(D_i|\theta, I_{jk})\, p(\theta|I_{jk})}{\int p(D_i|\theta, I_{jk})\, p(\theta|I_{jk})\, d\theta}. \tag{4}$$

The prior distribution $p(\theta|I_{jk})$ represents our initial knowledge about the probability of the performance index being in its region of acceptance. Since, we may have little knowledge about the performance of system that is being tested, we can chose a uniform prior:

$$p(\theta|I_{jk}) = 1, \qquad 0 \le \theta \le 1. \tag{5}$$

With this prior, and the sampling distribution (3), the posterior (4) can be determined analytically [7]:

$$p(\theta|D_i, I_{jk}) = \frac{(N+1)!}{R!(N-R)!}\theta^R (1-\theta)^{N-R}. \tag{6}$$

3.2 Prediction

Having computed the posterior of the probability of success of a particular index, the question that arises is what is the actual probability of obtaining a certain number of successes in a certain number of future missions? If we knew the true success probability θ, then the probability of having Z successes in M missions is given by the Binomial distribution:

$$p(Z|\theta) = \binom{M}{Z} \theta^Z (1-\theta)^{M-Z}. \tag{7}$$

In practice we only know the posterior (6) and not the actual value of θ. So the predicted probability of Z given the data D_i can be computed from

$$p(Z|D_i, I_{jk}) = \int_0^1 p(Z|\theta)\, p(\theta|D_i, I_{jk})\, d\theta. \tag{8}$$

By doing this integration, we average the uncertainty about θ.

The coverage probabilities in (2), are the predicted probabilities of one success in the next mission. These can be computed by taking Z=1 and M=1 in (7), in which case (8) reduces to

$$\begin{aligned} p(S_i|D_i, W_k, F_k, I) &= \int_0^1 \theta\, p(\theta|D_i, I_{jk})\, d\theta, \\ &= \frac{R+1}{N+2}. \end{aligned} \tag{9}$$

From the sampling distribution (6), the coverage reduces to

$$p(S_i|D_i, W_k, F_k, I) = \frac{R+1}{N+2}.$$

4 A Single Figure of Merit

In some cases, it may be convenient to have a single figure of merit for robust autonomy. The natural procedure to obtain this figure would be to evaluate the probability that all the indices are jointly within their regions of acceptable performance, namely,

$$\begin{aligned} &P(S_1, \ldots, S_l|D, I) \\ &\quad = \sum_j \sum_k P(S_1, \ldots, S_l, W_j, F_k|D, I) \\ &\quad = \sum_j \sum_k P(S_1, \ldots, S_l|W_j, F_k, D)\, P(W_j|I) P(F_k|I). \end{aligned}$$

5 Example of Computations

In this section, we consider an example, of a test in simulation, of an autopilot part of a remotely piloted aircraft system with a capability for control surface fault detection and control reconfiguration [9]. The UAS has a mass of 28Kg and is to be considered for surf-condition monitoring at 1km off the coastline. This aircraft has four control surfaces, ailerons and split elevators, to create redundancy to servo failures via control allocation.

We consider the part of the mission related to approaching a recovery location (before the landing phase). The desired trajectory is shown in Figure 2. The assumed weather conditions are given by a mean wind speed and turbulence spectrum [10], and faults in the four control surface servos are also considered. The operational conditions for testing and their associated marginal probabilities are summarised in the following:

F_0: Healthy; $P(F_0|I) = 0.7619$.

F_1: Right aileron; $P(F_1|I) = 0.0794$.

F_2: Left aileron; $P(F_2|I) = 0.0794$.

F_3: Right elevator; $P(F_3|I) = 0.0397$.

F_4: Left elevator; $P(F_4|I) = 0.0397$.

W_1: Wind 0 knots; $P(W_1|I) = 0.0909$.

W_2: Wind 10 knots; $P(W_2|I) = 0.6364$.

W_3: Wind 20 knots; $P(W_3|I) = 0.2727$.

To evaluate performance we consider the indices shown in Table 2. The time at which the faults occur is assumed to be uniformly distributed over the length of the mission.

The evaluations of the coverage probabilities $P(S_i|W_j,F_k,D,I)$, are summarised in Table 3. Each probability is computed using (9) and data of 100 simulation scenarios. Figure 3, for example shows the outcomes of the simulation for the index related to the bank angle for the case of wind of 10kts and no fault; that is predicted coverage $P(S_1|W_2,F_0,D,I) = 0.9820$ in Table 3.

Table 2 Performance indices and limits for the tested mission.

Index	Description	Limits
r_1	Bank angle	$\pm$60deg
r_2	Loading factor	$\pm$3.5
r_3	Angle of attack	$\pm$11.5deg
r_4	Air speed	$<$ 30m/s
r_5	Horiz Pos Error	$\pm$5m
r_6	Vert Pos Error	$\pm$5m

Figure 3 also shows the posterior $p(\theta|D_1,I_{10})$, where $I_{10} = \{W_1,F_0,I\}$, computed using (6). Figure 4 shows the outcomes and posterior for the case bank angle for the case of wind of 10kts and fault in the right aileron, that is predicted coverage $P(S_1|W_2,F_1,D,I) = 0.9310$ in Table 3.

Using the probabilities in Table 3 into (2), we obtain the following measures of robust autonomy:

- $P(S_1|D,I) = 0.9737$ (Bank angle)
- $P(S_2|D,I) = 0.9737$ (Loading factor)
- $P(S_3|D,I) = 0.9806$ (Angle of attack)
- $P(S_4|D,I) = 0.9820$ (Air speed)
- $P(S_5|D,I) = 0.7600$ (Horiz Pos Error)
- $P(S_6|D,I) = 0.8208$ (Vert Pos Error)

As we can see from these figures, the performance of fault-tolerant autopilot is satisfactory for most performance indices except for the location relative to the desired trajectory, which for this part of the mission has stringent tolerances as specified in Table 2.

To assess what the main limiting issues may be, we can analyse the coverage probabilities shown in Table 3. Figure 5 shows a graphical display of these probabilities. These data indicate that the system handles very well the various faults and environmental conditions for the first four performance indices (bank angle, loading, factor, AoA, and air speed) with a probability above 0.9 of being inside the region of acceptable

performance. The location indices struggle under faults and the degradation of performance is increases with the severity of the weather. For a discussion on how this data can be used for certification and also to improve initial system see our companion paper [2].

Table 3 Coverage Probabilities $P(S_i|W_j,F_k,D)$

S_1	F_0	F_1	F_2	F_3	F_4
W_1	0.9820	0.9410	0.8920	0.9820	0.9820
W_2	0.9820	0.9310	0.9310	0.9820	0.9820
W_3	0.9820	0.9410	0.9410	0.9590	0.9680
S_2	F_0	F_1	F_2	F_3	F_4
W_1	0.9820	0.9410	0.8920	0.9820	0.9820
W_2	0.9820	0.9310	0.9310	0.9820	0.98202
W_3	0.9820	0.9410	0.9410	0.9590	0.9680
S_3	F_0	F_1	F_2	F_3	F_4
W_1	0.9820	0.9500	0.9216	0.9820	0.9820
W_2	0.9820	0.9820	0.9680	0.9820	0.9820
W_3	0.9820	0.9820	0.9820	0.9820	0.9820
S_4	F_0	F_1	F_2	F_3	F_4
W_1	0.9820	0.9820	0.9820	0.9820	0.9820
W_2	0.9820	0.9820	0.9820	0.9820	0.9820
W_3	0.9820	0.9820	0.9820	0.9820	0.9820
S_5	F_0	F_1	F_2	F_3	F_4
W_1	0.9820	0.9750	0.9750	0.9820	0.9820
W_2	0.8450	0.8030	0.7940	0.7050	0.7840
W_3	0.6820	0.0180	0.0180	0.0180	0.0180
S_6	F_0	F_1	F_2	F_3	F_4
W_1	0.9820	0.9750	0.9750	0.9820	0.9820
W_2	0.8450	0.8030	0.7940	0.7050	0.7840
W_3	0.7820	0.7180	0.6180	0.6180	0.5180

5.1 Simulation Scenarios and Quality of the Estimates

A point estimate of θ (the probability of a success of a performance index in a mission) can be taken as the value of θ at which the posterior (6) is maximum θ_{MAP} (maximum a posteriori). By taking the logarithm of the posterior

$$L = \log p(\theta|D_i,I_{jk}), \tag{10}$$

and using a second-order Taylor expansion, it is shown in [8], that the 95% confidence interval of that covers the true value is given by $[\theta_{\text{MAP}}-2\sigma,\theta_{\text{MAP}}+2\sigma]$, where

$$\sigma = \left(\frac{d^2L}{d\theta^2}\bigg|_{\theta_{\text{MAP}}}\right)^{-1/2} = \sqrt{\frac{\theta_{\text{MAP}}(1-\theta_{\text{MAP}})}{N}}. \tag{11}$$

As discussed [8], the value of θ_{MAP} does not change very much after a moderate amount of data is used. The maximum of the numerator in (11) is attained for θ_{MAP} =0.5. This indicates that it requires more data to estimate the parameter θ for a system with medium performance ($\theta_{\text{MAP}} \approx 0.5$) than for a system with either very good performance ($\theta_{\text{MAP}} \approx 1$) or very bad performance ($\theta_{\text{MAP}} \approx 0$). In the example of the previous section, we used 100 scenarios, which means that for the worst case, the true value of θ will be in the interval $\theta_{\text{MAP}} \pm 0.1$.

The number of simulations required to achieve a desired quality level in the estimates can required quite a few hours of hardware-in-the loop simulation. This can be alleviated by testing in parallel different sections common to many missions. This may require, for example, to consider different weather conditions and faults for

- take off,
- climbing to mission altitude,
- manoeuvring at altitude,
- sense and avoid,
- approach to recovery,
- landing.

6 Conclusions

This paper refines a previously proposed framework for a probabilistic assessment of various degrees of robust autonomy in UAS. The probabilistic assessment takes into account uncertainty in the weather conditions and fault scenarios under which the UAS autonomous decision making must operate. Data collected from testing, potentially using hardware-in-the-loop simulations provides information about coverage, namely, the probability that the system will keep adequate

levels of performance given a particular weather and fault conditions. The coverage probabilities are then used to compute measures of robust autonomy, which are selected according to the requirements of the mission and airframe capabilities. These measures are probabilities of satisfactory performance given what has been learned through the system evaluation. The evaluation of performance is done without specific knowledge of the implementation of autonomous decision making.

The proposed framework provides the probabilities that are the basis necessary for decision making by the NAAs. If an NAA adopts the proposed framework, then regulations for certification of classes of missions should detailed the required levels or reliability of robust autonomy required.

References

[1] Dalamagkidis, K., Valavanis, K., and Piegl, L., *On Integrating Unmanned Aircraft Systems into the National Airspace system*, Intelligent systems, control and automation, science and engineering, Springer, 2009.

[2] Perez, T., B. Williams and P. de Lamberterie "Evaluation of Robust Autonomy and Implications on UAS Certification and Design" 28th International Congress of the Aeronautical Sciences ICAS, Brisbane, Australia, 2012.

[3] Perez, T., A. Donaire, P. de Lamberterie, B. Williams "A Framework for Testing Robust Autonomy of UAS During Design and Certification" Proc of AIAA Infotech Aerospace Conference, March, St Louis, Missouri USA, 2011.

[4] Perez, T., A. Donaire, and B. Williams, "On Evaluation of Robust Autonomy of Uninhabited Vehicles and Systems" In Proceedings of 7th IFAC Symposium on Intelligent Autonomous Vehicles. Sept., Lecce, Italy, 2009.

[5] Rausand, M. and Høyland, A., *System Reliability Theory: Models, Statistical Methods and Applications*, Wiley Interscience, second edition ed., 2004.

[6] Wu, E. "Coverage in Fault-tolerant Control" Automatica (40), p. 537-548, 2004.

[7] Jaynes, E.T. *Probability Theory - The Logic of Science*. Cambridge University Press. 2003.

[8] Sivia, D.S and J. Skillling *Data Analysis - A Bayesian Tutorial*. Oxford Science Publications. 2006.

[9] de Lamberterie, P. and T. Perez and A. Donaire, "A Low-complexity Flight Controller for Unmanned Aircraft Systems with Constrained Control Allocation" In Proceedings of the Australian Control Conference, Melbourne, 2011.

[10] Keegan, W. B. "Terrestrial environment (climatic) criteria handbook for use in aerospace vehicle development." Technical Report NASA-HDBK-1001, Nasa Technical Standards Program, 2000.

6.1 Copyright Statement

The authors confirm that they, and/or their company or organisation, hold copyright on all of the original material included in this paper. The authors also confirm that they have obtained permission, from the copyright holder of any third party material included in this paper, to publish it as part of their paper. The authors confirm that they give permission, or have obtained permission from the copyright holder of this paper, for the publication and distribution of this paper as part of the ICAS2012 proceedings or as individual off-prints from the proceedings.

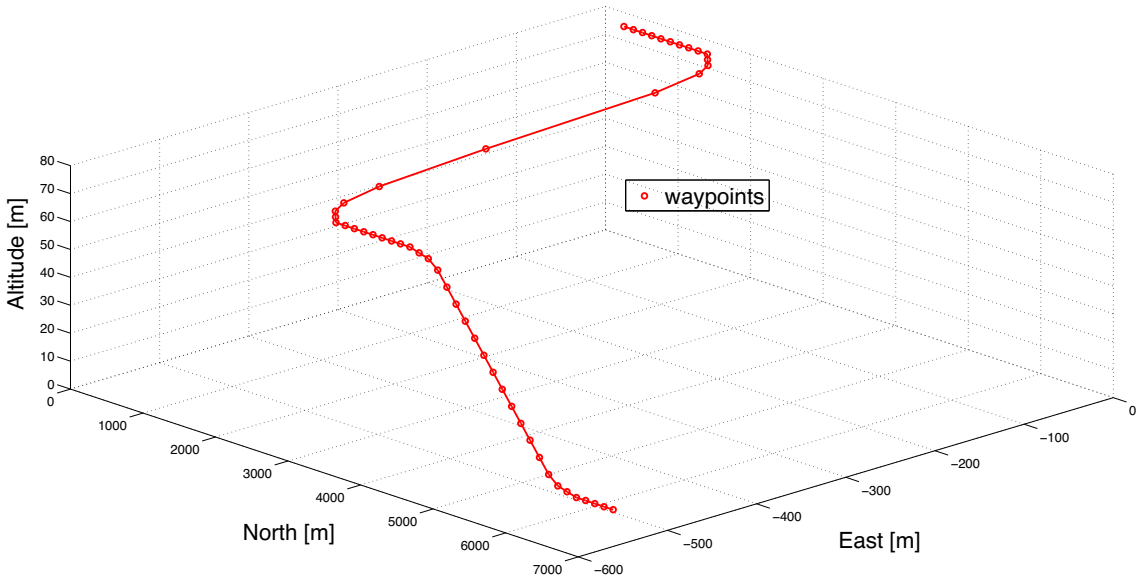

Fig. 2 Desired trajectory for approaching a recovery location.

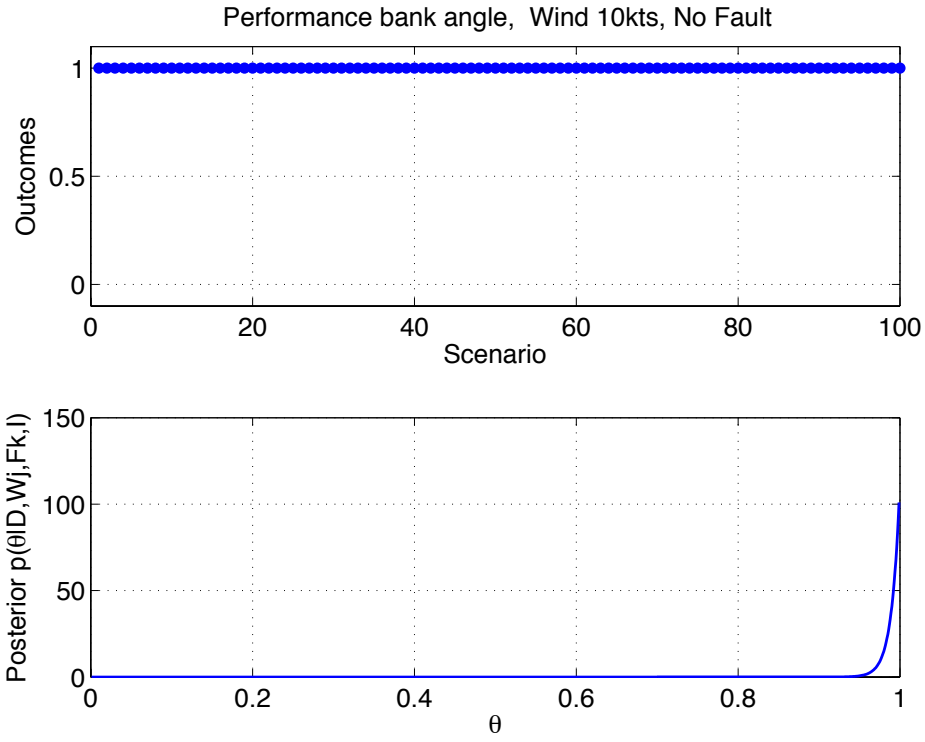

Fig. 3 Simulation outcomes and posterior for bank angle with a wind of 10kts and no fault.

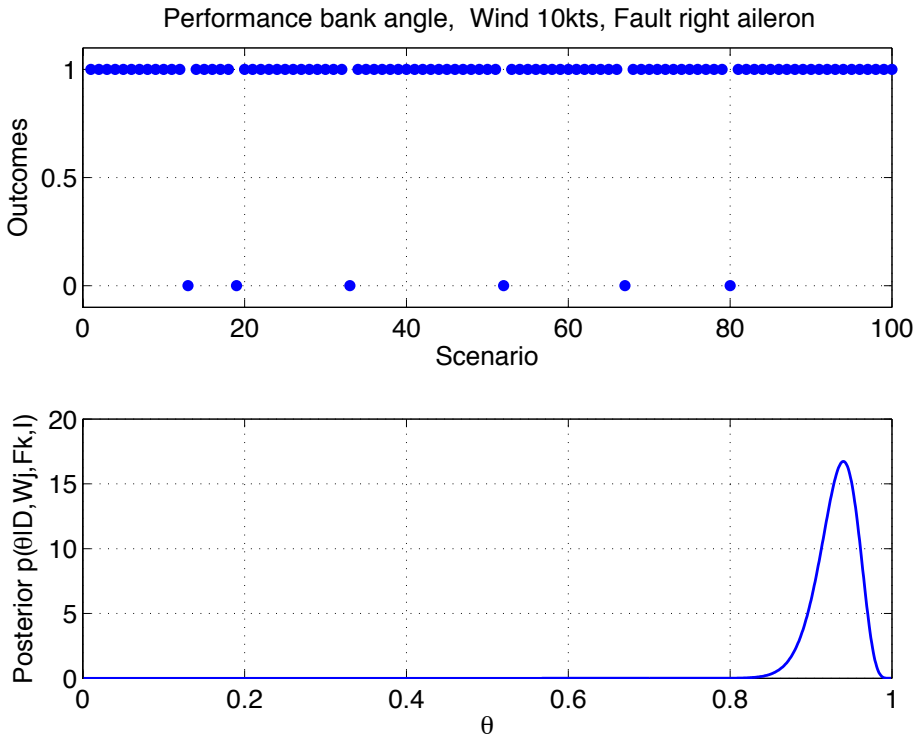

Fig. 4 Simulation outcomes and posterior for bank angle with a wind of 10kts and a fault in the right aileron.

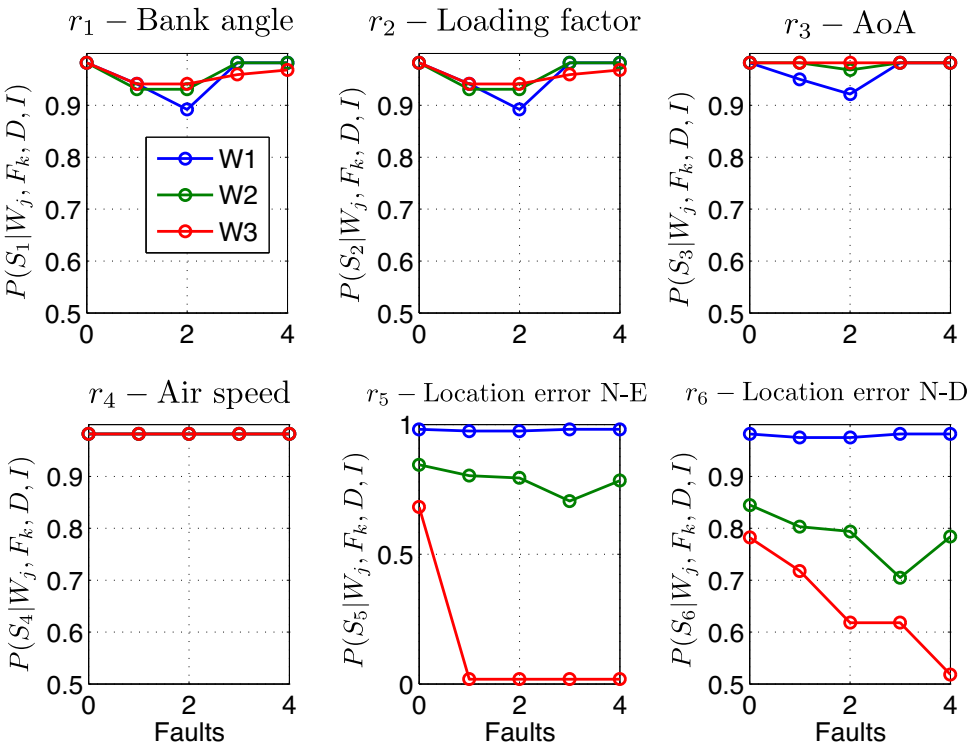

Fig. 5 Coverage probabilities.